Analysis of Human Neck Loads During Isometric Voluntary Ramp Efforts: EMG-Assisted Optimization Modeling Approach

Hyeonki Choi

Division of Orthopedic Surgery and Department of Mechanical Engineering University of Wisconsin-Madison, USA

Neck muscle forces and spinal loads at the C4/5 level were estimated that result from isometric voluntary ramp efforts gradually developing to maximums in flexion, extension, left lateral bending and right lateral bending. Electromyographic (EMG) activities, a three-dimensional anatomic data of the neck and a hybrid model, EMG-assisted optimization (EMGAO) model, were used. The model computed the cervical loads at 25%, 50%, 75%, and 100% of peak moments. The highest model-predicted C4/5 joint compressive forces occurred during flexion; 361 (±164) N, 811 (±288) N, 1207 (±491) N and 1674 (±319) N in 25%, 50%, 75% and 100% of peak moment respectively. Variations in load distribution among the agonistic muscles and co-contractions of antagonistic muscles were estimated during ramp efforts. Results suggest that higher C4/5 joint loads than previously reported are possible during isometric, voluntary muscle contractions. These higher physiological loads at C4/5 level must be considered possible during orthopedic reconstruction at this level.

Key Words : Cervical Loads, EMG-Assisted Optimization, Isometric Ramp Effort

Nomenclature

f_j : *ith* muscle force (N)

emg/emg_{max} : Muscle activation level expressed as a fraction of its maximum EMG activity

a_i : *ith* muscle cross-sectional area (m^2)

σ_{max} : Maximum muscle force generated per unit of cross-sectional area (3.5×10^5 N/m^2)

M_{emg_x}, M_{emg_y}, M_{emg_z} : Intermediate estimated moments acting on the joint about x, y and z

f_{xi}, f_{yi}, f_{zi} : Estimated individual muscle forces of *ith* muscle in the x, y and z joint axes

r_{xi}, r_{yi}, r_{zi} : Muscle moment arms of *ith* muscle with respect to the x, y and z joint axes

n : Number of muscles crossing a given joint

G : Common muscle gain

M_x, M_y, M_z : Total moments necessary to balance moments acting on the joint about x, y and z

M_{emg_i} : Intermediate estimated moment which the *ith* muscle produces about a joint

g_i : *ith* individual muscle gain

$M_{emg_{xi}}$, $M_{emg_{yi}}$, $M_{emg_{zi}}$: Intermediate estimated individual muscle moments about x, y and z

RMS_{error} : Root mean square (RMS) errors of the model predicted moments

n_t : Number of trials

M_{mean} : Measured external moment

M_{emgao} : EMGAO model-predicted external moment

E-mail : h-choi@nwu. edu
TEL : +1-312-503-0799 ; **FAX** : +1-312-503-5101
Department of Physiology, Northwestern University, Medical School, 303 E. Chicago Ave., Chicago, IL 60611, USA (Manuscript **Received** August 23, 1999; **Revised** November 9, 1999)

1. Introduction

Human neck is particularly susceptible to

injury due to its structural weakness with large mass of head sitting on the top of flexible cervical spine column. Mechanical factors are generally involved in the cause of some neck pain. A detailed information of the neck muscle forces and spinal loads imposed by the performance of physical tasks will be useful to differentiate possible causes of neck pain.

The optimization technique is one of the typical approaches that are used to solve the statically indeterminant problem in biomechanical modeling of body segments (Kim and Pandy, 1998; Moroney et al., 1988; Schultz et al., 1983; Son and Miller, 1993). Although optimization models have proven useful in predicting muscle forces from intersegmental moments, some discrepancies between model predictions and empirical results exist. For example, some coefficients of linear correlation between predictions of a neck model and experimental results were 0.29 and 0.33 (Moroney et al., 1988). A major weakness of optimization models is that they do not predict co-contraction of antagonistic muscles, yet the co-contraction of muscles developing opposing moments about a joint is a common experimental observation (Marras, 1988). The optimization models often predict muscles to be inactive in situations where significant EMG activity is observed (Ladin et al., 1989; Schultz et al., 1982a; Schultz et al., 1982b; Schultz et al., 1987).

The EMG-based approach, on the other hand, predicts co-contractions of antagonistic muscles together with the various patterns of agonistic synergy (McGill, 1992). The EMG-based approach is sensitive to subject and trial differences in the magnitudes of individual muscle forces needed to produce the same reaction moment, while the optimization method shows a similar estimate of muscle forces for all subjects and trials producing the same moment. In several studies, EMG-based strategy was used to estimate forces in active tissues in a lumbar spine model (McGill and Norman, 1986; McGill, 1992; McGill, 1991).

Cholewicki and McGill (1994) introduced a new technique termed 'EMG-assisted optimization' (EMGAO). This new hybrid approach provided physiologically based muscle recruitment patterns and satisfied the exact fulfillment of moment constraints about three orthogonal joint axes. A companion paper of this study (Choi and Vanderby, 1999) showed that the EMGAO approach is an improvement over both the conventional EMG-based and optimization methods in musculoskeletal modeling of human neck because of its capability of balancing moments and sensitivity to small variation in muscle response.

In this study, we calculated the muscle forces and spinal loads of human neck during isometric ramp efforts that were gradually developed to maximum exertions in extension, flexion, left and right lateral bending. For this purpose, an EMAGO model was formulated and electromyographic experiments were conducted. Following hypotheses were tested in this study: (i) the EMGAO model predicts various muscle force distribution patterns including antagonistic co-contractions during isometric ramp efforts; (ii) the EMGAO model predicts cervical spinal compressive loads which are higher than previous report (Moroney, 1988) that did not include antagonistic muscle forces during isometric ramp efforts.

2. Methods

2.1 Experimental design

Ten healthy male volunteer subjects (mean age $\pm$SD: 31.2$\pm$2.0 years) who had no history of neck injury or notable neck pain participated in the experiment. The subjects were asked to sit in a chair, and then their upper body and arms were tied with Velcro® strap to a board fixed behind the chair with their hands placed on their laps. A head-band (made with Velcro® strap) was worn by each subject, and the head band was connected with a rope to a fixed force transducer.

The EMG signals were measured with eight pairs of bipolar Ag-AgCl surface electrodes (diameter of disc, 6 mm; Grass Instruments, Quincy, Mass, USA) affixed around the neck at the C4/5 level. The C4/5 level of the neck was located by palpation of the vertebrae. The eight

electrode locations were denoted as anterior, anterolateral, posterolateral, and posterior, bilaterally. Their locations approximated azimuth angles of 35° 70° 105° and 150° respectively; midway between the anterior midline and the anterior border of the sternocleidomastoid (SCM) muscle; midway between the anterior and posterior borders of the SCM muscle; midway between the posterior border of the SCM muscle and anterior border of the upper trapezius muscle; midway between the anterior border of the upper trapezius muscle and the posterior midline (Moroney, 1988).

After the electrodes were affixed, each subject performed two sets of isometric tasks calling for neck muscle contractions. The first set of tasks consisted of maximum isometric efforts to produce the largest amplitudes of EMG activity from the selected neck muscles to provide a basis for normalization. For this purpose two basic isometric restraint strategies were used in which subjects attempted to produce maximum muscle activity. The first strategy consisted of maximum isometric exertions while sitting on a restraint chair. The upper body was fixated to the chair, and the head was restrained by a cord and head strap from a fixed wall. Then, extension, flexion, left lateral bending and right lateral bending efforts were performed with resistance supplied by the wall. The second strategy was to record muscle activity during maximum isometric rotation efforts. These rotation efforts were performed with the head in neutral position, 30° pre-rotated to the left and 30° pre-rotated to the right with the body and neck in an upright posture. An assistant provided a matching resistance to the subject's head during the maximum rotation effort. During the first set of tasks, loads were measured for extension, flexion, lateral bendings but rotation loads were not measured. Three trials were collected during the first set. The largest EMG activity observed during any of these strategies was taken as 100% maximum voluntary contraction (MVC) for each particular muscle.

In the second set of tasks, subjects performed near maximum, isometric, voluntary, and ramp efforts in extension, flexion, left lateral bending, and right lateral bending. Each subject was instructed to gradually build up to maximum efforts, peaking at about 5 seconds. Three trials of each effort were performed. During the second set, all loads were measured by a fixed force transducer. In total, each subject performed 42 isometric quasi-static tasks. A two-minute recovery period was allowed between contractions to avoid fatigue. A schematic of the testing procedure is given in Fig. 1.

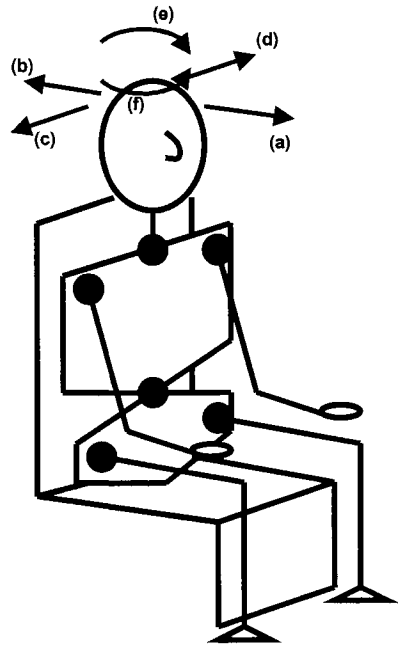

Fig. 1 Schematic diagram of testing procedure for MVC showing (a) attempted extension effort (b) attempted flexion effort (c) attempted left lateral bending effort (d) attempted right lateral bending effort (e) attempted counter-clockwise twisting effort (f) attempted clockwise twisting effort. Each arrow indicates direction of resistance

The EMG signals were pre-amplified, further amplified, full-wave rectified, low pass filtered (cutoff frequency: 3 Hz) (using Grass Instrument, Quincy, Mass, USA), and A/D converted (100 Hz) sequentially. Finally, the digitized signals were saved to a personal computer. Signals from the force transducer were fed to an amplifier, A/D converter (100 Hz), and then saved to the computer. Measured external loads and the esti-

mated weights of the subjects' heads were used as input values of the model. The weight of the head was assumed to be 7.3% of the subject's total body weight with a center of mass acting midway between the ears (Clauser et al., 1969).

2.2 Biomechanical human neck model

To construct the human neck model, the origin of an orthogonal coordinate system was located at the disc center of the C4/5 level. Positive directions were chosen as the left, posterior and superior. In this model, the C4/5 motion segment resisted only compressive and shear forces, but no bending or twisting moments. This assumption is similar to that used in lumbar trunk model of Schultz and Andersson (1981) and in a cervical model of Moroney et al. (1988). In this study, anatomical data of the neck model reported by Moroney et al. (1988) was used. Muscle centroidal coordinates were expressed relative to the frontal and sagittal plane neck diameters, and their areas were scaled relative to the product of the diameters.

In this study, 14 pairs of muscles (28 muscles) were modeled and grouped to correspond to eight electrode sites. The grouping of the muscles is based on the assumption that muscles in the same group experience the same EMG activities as a percent of MVC. Bilateral grouping of muscles is as follows: *Anterior*: Platysma, Infrahyoid; *Anterolateral*: Sternocleidomastoid, Longus colli and cervicis, Scalene anterior; *Posterolateral*: Scalene medius, Longissimus cervicis, Levator scapulae, Splenius cervicis; *Posterior*: Multifidus, Semispinalis cervicis, Semispinalis capitis, Splenius capitis, Trapezius.

2.3 EMG-assisted optimization (EMGAO) modeling procedure

In the first step of the EMG-assisted optimization modeling procedure, each EMG signal was normalized by the maximum EMG activity that was observed at that site during any of the test postures that are shown in Fig. 1. Then, with these normalized EMG values and EMG-muscle force relationship, the initial assignment of muscle forces was made on a spreadsheet (Quattro Pro 6.0, Novell, Inc.). Muscle forces were assumed to have a power relationship with the mean rectified EMG signal expressed as a fraction of MVC based on the data of Stokes et al. (1987), and Vink et al. (1987). Cholewicki et al. (1995) also supported this non-linear relationship from their experiment.

$$f_i=\left(\frac{emg}{emg_{max}}\right)^{1/1.3} a_i\sigma_{max} \tag{1}$$

where f_i is the *ith* muscle force (N); a_i is the *ith* muscle cross-sectional area (m^2); σ_{max} is the maximum muscle force generated per unit cross-sectional area (3.5×10^5 N/m^2); emg/emg_{max} is the muscle activation level expressed as a fraction of its maximum EMG activity (Cholewicki et al., 1995). The passive force was neglected for this isometric experiment.

In the second step, a common gain (G) is introduced to compensate for overall systematic errors in the initial assessment of muscle forces (Cholewicki et al., 1995). The common gain for all muscle was calculated by using a least mean square regression fitting the model predictions and measured moments:

$$\begin{aligned} Memg_x&=\sum_{i=1}^{n}(r_{yi}f_{zi}-r_{zi}f_{yi}),\quad n=28\\ Memg_y&=\sum_{i=1}^{n}(r_{zi}f_{xi}-r_{xi}f_{zi}),\quad n=28\\ Memg_z&=\sum_{i=1}^{n}(r_{xi}f_{yi}-r_{yi}f_{xi}),\quad n=28 \end{aligned} \tag{2}$$

$$\sum_{k=x,y,z}(GMemg_k-M_k)^2=min. \tag{3}$$

where M_x, M_y, M_z are total moments necessary to balance moments acting on the joint about x, y and z axes; G is common gain; f_{xi}, f_{yi}, f_{zi} are estimated individual muscle forces in the x, y, and z joint axes directions, respectively; r_{xi}, r_{yi}, r_{zi} are muscle moment arms with respect to the x, y and z joint axes; M_{emg_x}, M_{emg_y}, M_{emg_z} are the total moment estimated from muscles acting on the joint about x, y and z axes. The common gain value, G, was calculated on MATLAB (MATLAB V4.2c. 1, The MathWorks, Inc.). After the gain value was obtained, the second set of the muscle forces was obtained by multiplying the initial set of muscle forces to the common gain value.

In the third step, an objective function is formed to balance all three moments acting about the joint by applying the least possible adjustment to individual muscle force that was obtained from the second step. This process is implemented by altering the individual muscle gains. This can be formulated as follows:

$$\sum_{i=1}^{n} M_{emg_i}(1-g_i)^2 = min.,$$
$$M_i = \sqrt{M^2_{emg_{xi}} + M^2_{emg_{yi}} + M^2_{emg_{zi}}} \quad (4)$$

subject to

$$\sum_{i=1}^{n} g_i M_{emg_{xi}} = M_x,\ \sum_{i=1}^{n} g_i M_{emg_{yi}} = M_y,$$
$$\sum_{i=1}^{n} g_i M_{emg_{zi}} = M_z \quad (5)$$
$$g_i \geq 0,\ i=1, 2, \cdots, n \quad (6)$$

where n is the number of muscles crossing a given joint; g_i is the individual muscle gain; M_{emg_i} is the estimated moment which the ith muscle produces about the joint center of rotation (geometric sum of $M_{emg_{xi}}$, $M_{emg_{yi}}$ and $M_{emg_{zi}}$); $M_{emg_{xi}}$, $M_{emg_{yi}}$ and $M_{emg_{zi}}$ are the estimated individual muscle moments about the x, y, and z joint axes, respectively; M_x, M_y, M_z are total moments necessary to balance moments acting on the joint about x, y and z axes. The non-linear objective function requires that the individual gain, g_i, be close to 1. 0 as unity leaves a muscle force unchanged. This non-linear approach forces the required gain adjustments on all muscles rather than on one or just a few muscles (Cholewicki et al., 1995). After the individual gain values were obtained, the final set of the muscle forces was obtained by multiplying each muscle force of the second set to the corresponding individual muscle gain value.

To test the accuracy of the model predictions, root mean square (RMS) errors of the model predicted moments were calculated. The RMS error is defined as following:

$$RMS_{error} = \sqrt{\frac{1}{n_t}\sum_{i=1}^{n_t}\left(\frac{M_{emgao_i} - M_{meas_i}}{M_{meas_i}}\right)^2} \quad (7)$$

where n_t is the number of trials; M_{meas} is the measured external moments; M_{emgao} is the model predicted external moments. If the measured external moments are identical with model predicted moments, the RMS error is equal to zero. Any non-zero value of the RMS error indicates the difference between measured external moments and model-predicted moments.

3. Results

The relationships of external moments versus EMG (% MVC) (Fig. 2) were not consistently linear among subjects or between trials of subjects. Although, EMG signal amplitude generally increased with moment, the ramp loading did not always result in a smooth progression of the

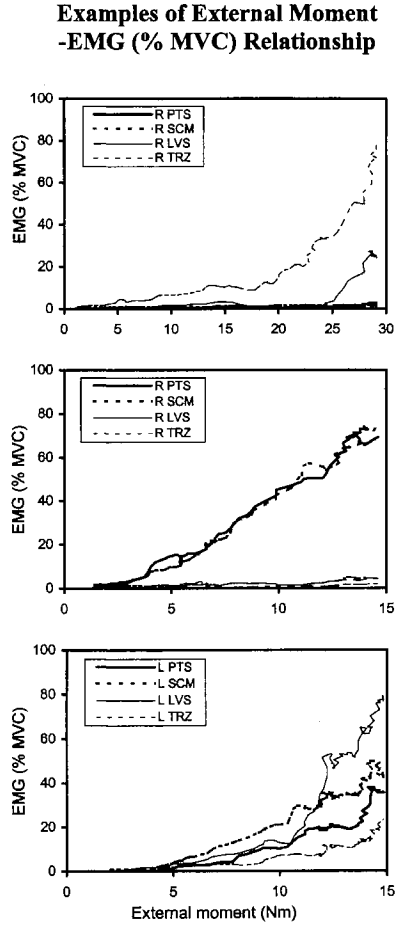

Fig. 2 Examples of external moment-EMG (% MVC) relationship developed during attempted extension (Subject 5, up), flexion (Subject 3, middle), left lateral bending (Subject 3, bottom). R: right side, L: left side, PTS: platysma, SCM: sternocleidomastoid, LVS: levator scapulae, TRZ: trapezius

EMG activity. In flexion, agonistic muscles (platysma and sternocleidomastoid) showed a consistent linear behavior across the subjects and trials. The external moment versus EMG (% MVC) graph shows how the EMG signal developed in the antagonistic muscles. Near maximal moments, co-contraction increased significantly. Compared to the other efforts, lateral bending produced the highest EMG signal level in the antagonistic muscles.

There were consistent trends of phasic relationships in muscle recruiting patterns. In extension, the trapezius becomes active earlier than levator scapulae. Levator scapulae showed a precipitous increase in activity from about three quarters of the whole ramp period. In flexion, the agonists (platysma, SCM) showed similar phasic patterns. These agonist muscles become active early and remained active throughout the whole ramp period. In lateral bending, all of the muscles (agonists, antagonists) became active in the exertions.

Table 1 Mean(±SD) muscle forces(N) computed by the EMGAO model during peak attempted extension, flexion, left lateral bending, and right lateral bending moments, averaged across subjects, standard deviations in parentheses

Mean Muscle Forces Computed by the EMGAO Model

Muscle Equivalents	Computed muscle forces(N)			
	Extension	Flexion	L Lat Bend	R Lat Bend
L Platysma	2(±1)	55(±11)	47(±8)	10(±3)
R Platysma	2(±1)	51(±15)	7(±4)	43(±7)
L Infrahyoid	6(±3)	181(±35)	113(±19)	62(±29)
R Infrahyoid	7(±3)	170(±50)	54(±22)	106(±20)
L Sternocleidomastoid	18(±6)	308(±97)	129(±31)	82(±47)
R Sternocleidomastoid	22(±12)	303(±102)	63(±37)	143(±17)
L Longus colli and cerv	4(±1)	60(±18)	48(±8)	19(±6)
R Longus colli and cerv	5(±2)	58(±19)	7(±6)	53(±13)
L Scalene anterior	6(±1)	79(±25)	69(±13)	21(±7)
R Scalene anterior	6(±3)	75(±26)	7(±5)	76(±21)
L Scalene medius	48(±18)	28(±15)	86(±29)	12(±3)
R Scalene medius	54(±14)	30(±12)	6(±3)	69(±16)
L Longissmus cerv	32(±12)	16(±8)	43(±14)	16(±6)
R Longissimus cerv	35(±8)	17(±7)	7(±3)	36(±10)
L Levator scapulase	125(±57)	70(±35)	155(±53)	13(±9)
R Levator scapulae	134(±34)	76(±32)	18(±11)	133(±42)
L Multifidus	48(±10)	8(±5)	5(±2)	14(±3)
R Multifidus	52(±10)	10(±5)	10(±5)	4(±3)
L Semispinalis cerv	97(±22)	16(±11)	34(±12)	10(±6)
R Semispinalis cerv	92(±27)	19(±11)	7(±5)	33(±19)
L Semispiinalis cap	132(±29)	22(±15)	72(±22)	9(±7)
R Semispinalis cap	126(±33)	27(±14)	7(±5)	77(±20)
L Splenius cervicis	22(±7)	8(±4)	26(±6)	3(±1)
R Splenius cervicis	23(±5)	9(±4)	3(±2)	21(±7)
L Splenius capitis	58(±14)	11(±7)	54(±17)	3(±3)
R Splenius capitis	62(±17)	13(±7)	6(±1)	63(±25)
L Trapezius	74(±17)	45(±13)	13(±8)	12(±6)
R Trapezius	71(±18)	49(±15)	11(±6)	19(±14)

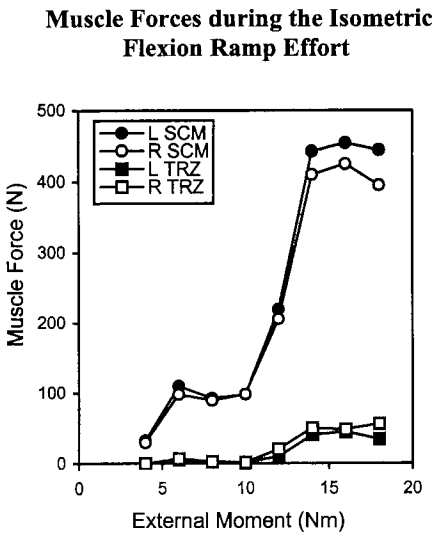

Fig. 3 Example of predicted forces of selected muscles from the model during the isometric flexion ramp effort (subject #1). Left and right SCM represent agonists and left and right TRZ represent antagonists. L SCM: Left Sternocleidomastoid, R SCM: Right Sternocleidomastoid, L TRZ: Left trapezius, R TRZ: Right trapezius

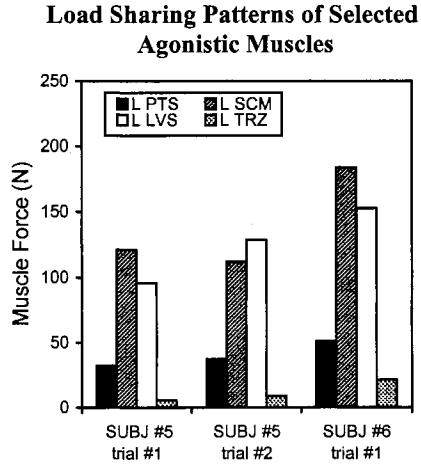

Fig. 4 Example of load sharing patterns of selected agonistic muscles from the model between subjects and between trials of the same subject during attempted left lateral bending effort. L PTS: Left platysma, L SCM: Left sternocleidomastoid, L LVS: Left Levator scapulae, L TRZ: Left trapezius

Table 1 shows the mean (across subjects) muscle forces predicted during peak moments. Mean (±SD) calculated neck muscle contraction forces ranged up to 308 (±97) N. The maximum muscle force occurred in the SCM during peak flexion exertions. Figure 3 shows an example of antagonistic co-contraction predicted by the model during a gradually developed isometric flexion trial. In flexion, left and right SCM constitute the agonists and left and right trapezius constitute antagonists. The model showed the maximal co-contraction of antagonist muscles in the vicinity of a peak moment as was seen from EMG behaviors expressed as a percent of MVC. The model shows various load distribution patterns among the agonist muscles even during the generation of moments of equal magnitudes, especially in lateral bending (Fig. 4). These variations existed not only between the subjects but also between the trials of the same subject.

Samples of each normalized EMG signal were selected for input into the model. Mean spinal loads during 25%, 50%, 75%, and 100% of the peak attempted efforts (lateral shear, anteroposterior shear, compressive force) are shown in Table 2. The mean (±SD) C4/5 joint compressive forces predicted during peak moments were 1386 (±203) N in extension, 1674 (±319) N in flexion, 989 (±239) N in left lateral bending, and 1061 (±185) N in right lateral bending. Generally, the shear forces were small in magnitude compared with compressive forces.

The mean (±SD) voluntary peak external moments developed by the 10 subjects were 28.3 (±3.3) Nm in extension, 17.7 (±3.1) Nm in flexion, 16.9 (±2.8) Nm in left lateral bending and 17.0 (±2.9) Nm in right lateral bending. The mean (±SD) model predicted peak moments about lateral, anteroposterior, and axial axes were respectively: 27.7 (±4.9) Nm, 0.6 (±0.3) Nm, and 0.1 (±0.1) Nm during extension; 17.0 (±4.1) Nm, 0 (±0.1) Nm, and 0.1 (±0.1) Nm during flexion; 0.4 (±0.3) Nm, 14.8 (±5.0) Nm, and 0.1 (±0.1) Nm during left lateral bending; 0.2 (±0.2) Nm, 14.6 (±5.4) Nm, and 0.1 (±0.2) Nm during right lateral bending. The RMS errors (%) of the model predicted moments about each corresponding axis were 2.1% in extension, 4.0% in flexion, 12.5% in left lateral bending, and

Table 2 Mean (±SD) predicted spinal loads (N) (compressive force lateral shear, anteroposterior shear) from EMGAO during attempted extension, flexion, left lateral bending, and right lateral bending efforts, averaged across trials and subjects. Standard deviations are in parentheses.

Mean Predicted Spinal Loads (Compressive Force, Lateral Shear, Anteroposterior Shear)

Spinal Loads	25%	50%	75%	100%
EXTENSION				
Compressive force	353(±57)	668(±104)	994(±171)	1386(±203)
Lateral Shear	−1(±6)	−4(±14)	−1(±7)	−6(±19)
A-P Shear	51(±8)	94(±9)	141(±17)	181(±27)
FLEXION				
Compressive force	390(±124)	746(±212)	1155(±267)	1674(±319)
Lateral Shear	1(±6)	7(±18)	−5(±16)	17(±21)
A-P Shear	19(±30)	70(±55)	118(±81)	171(±107)
L. LAT. BEND				
Compressive force	266(±98)	497(±149)	671(±180)	989(±239)
Lateral Shear	22(±11)	44(±13)	60(±23)	80(±33)
A-P Shear	11(±12)	23(±26)	16(±18)	68(±63)
R. LAT. BEND				
Compressive force	279(±119)	518(±137)	775(±155)	1061(±185)
Lateral Shear	−15(±9)	−32(±9)	−56(±17)	−73(±28)
A-P Shear	−1(±5)	0(±11)	11(±21)	49(±36)

14.2% in right lateral bending.

4. Discussion

The specific goals of this study were to determine neck muscle forces and spinal loads and to assess EMG activities of neck muscles that result from isometric ramp efforts. For this purpose, an EMGAO model was formulated and an EMG experiment was performed. The EMGAO model was able to predict antagonistic co-contractions and various muscle force distributions which corresponded to the muscle activation patterns during all the spans of isometric ramp efforts; thus hypothesis (i) is supported. The EMGAO model predicted spinal compressive loads which were higher than previous reports that do not include antagonistic muscle forces; thus hypothesis (ii) is supported by this study.

Observation of high levels of EMG activities as a percentage of MVC during maximum isometric rotation efforts is consistent with the results of Moroney et al. (1988). The high levels of EMG activities of cervical muscles in rotation may indicate that a primary role of neck musculature is rotation. This is in contrast to the reported EMG activities of lumbar muscles (McGill, 1991) where relatively high levels in bending and low levels in rotation suggested that bending is the primary role of lumbar musculature and rotation is secondary. These roles are confirmed by the orientation of the articular facets, restricting lumbar rotation, and allowing cervical rotation.

In the trapezius, it appeared that the starting position of rotation efforts affected the relative EMG level. A+30° pre-rotated starting position tended to increase the EMG level, and a−30° pre-rotated starting position tended to decrease the EMG level. This suggests that the starting position of rotation and hence the muscle or sarcomere length is related to the capability of muscle contraction. This high EMG activities are consistent with the muscle fiber directions of an agonists on one side which produces rotation, and the lower activity levels of their antagonistic counterparts. The recording of high level of EMG activity from the anterior and anterolateral electrodes on the side opposite the direction of rota-

tion is consistent with the observation of Moroney et al. (1988).

The EMG (% MVC)-moment relationship were not always smoothly linear. The relationship between EMG activity of an individual muscle and respective muscle force is limited because this relationship were formed between individual EMG activity and net moment that is the function of all agonist and antagonist muscles. Nevertheless, EMG activity makes it possible to assess the contribution of a corresponding muscle to a specific moment (McGill, 1991).

The cutoff frequency of the low pass filter (3 Hz) was selected based on the following. The frequency responses of the rectus femoris was reported to be between 1.0 and 2.8 Hz during walking (Olney and Winter, 1985), and approximately 3 Hz in the first dorsal interosseous (Milner-Brown et al., 1973). McGill (1992) reported that the 3 Hz cutoff in measuring dynamic lumbar spine muscle contractions produced an impulse of 53 ms, which is compatible with the 30-90 ms contraction times for various muscles (Butchthal and Schmalbruch, 1970). Generally, when the contractions change quasi-statically, as in many isometric experiments, the low pass filter cutoff frequency can be lower, even to 1 Hz (Hof, 1984).

The EMGAO model showed activation of all muscles including antagonistic co-contractions (Table 1; Figs. 2 and 3). The EMGAO approach also accommodated the variation of muscle force distribution patterns. Prediction of both muscle forces and muscle force distribution patterns are needed to understand the mechanisms of muscle recruitment strategies. The muscle force distribution patterns are especially critical when evaluating the effectiveness of an individual to avoid tissue failure and injury (Cholewicki et al., 1995) because individuals do alter their patterns of force distribution among the various muscles when performing repetitive tasks (Potvin and Norman, 1993).

The compressive loads calculated in this study were higher than previously indicated (Moroney et al., 1988) by approximately 11% in extension, 79% in flexion, and 16% in left lateral bending respectively during peak efforts. The large discrepancies in joint compressive force reflect differences in the predictions of the amount of antagonistic co-contractions (Table 2). Generally, the spinal compressive force indicates the extent of muscle co-contraction predicted by the model, and the variability reflects largely the individual difference in the muscle force distribution patterns (Cholewicki and McGill, 1994).

The effects of antagonistic muscle coactivation on lumbar spine stability and lumbar spine compression were estimated by using biomechanical lumbar spine models (Cholewicki et al., 1997; Gardner-Morse and Stokes, 1998; Thelen et al., 1995). Gardner-Morse and Stokes (1998) estimated the effects of antagonistic abdominal coactivation by calculating the muscle stresses, the maximum compressive loading on the lumbar spine, and the critical value of muscle stiffness parameter. They reported that antagonistic abdominal coactivation increased stability of the spine at the cost of a small increase in maximum spinal compression. Cholewicki et al. (1997) examined the coactivation of trunk flexor and extensor muscles. Their study demonstrated that the coactivation increased with added mass to the torso, and the coactivation was explained to provide the mechanical stability to the lumbar spine. Thelen et al. (1995) suggested that substantial contractions of lumbar muscles, especially during asymmetric exertions, are used for increasing stability at the L3-L4 level. Our results of antagonistic co-contractions and higher maximal compressive loads also suggest that antagonistic neck muscle co-contractions are necessary to provide stability to the human cervical spine around its neutral posture by stiffening the joint.

Maiman et al. (1983) tested whole cervical spinal columns (skull-T3) for failure using compressive loads applied at the vertex. They applied compressive loads 2 cm posterior and 1 cm anterior to the vertex to simulate flexion and extension. They reported average axial loads at failure as 3567 N with no pre-flexion and 1823 N with pre-flexion. Shea et al. (1991) reported the strength of the lower cervical spine (C5-T1) as 2158 N in compressive force. Considering these

reports on spinal strength in compression, all of the maximal mean C4/5 joint compression force predicted from the model, 1674 N, is below the spinal strength and hence do not violate physiologic constraints. The spinal loads calculated in this study are, however, in a range that could possibly cause tissue damage at pre-failure loads based upon some ex vivo experiments. It must be also borne in mind that tests herein were done on young healthy males whereas most ex vivo testing is on older spines with less bone density and more structural compromise. In addition, ex vivo testing does not accurately simulate boundary conditions, muscle loading, etc.

The most significant limitation of the experiment resulted from measuring EMG activity with surface electrodes. As such they could have been affected by cross-talk from signals of different muscles. Vink et al. (1989) quantified cross-talk between electrodes by using 12 pairs of bipolar surface electrodes over the erector spine group during isometric contractions. They reported that the absolute maximum in the correlation coefficient was less than 0.3 when electrode pairs were placed more than 30 mm apart. And they concluded that even at the small distance of 30 mm between electrode pairs, EMG signals are specific and optimize selective recording of localized muscle activity in the erector spinae. In this study, the distance between the electrode pairs was greater than 30 mm to minimize cross-talk between electrodes during exertions. Even though electrode pairs were placed more than 30 mm apart, there is still EMG crosstalk effects from underlying muscles. This may explain why the EMG behaviors for the more anterior muscles (sparse muscle area) were closer to linear than for the more posterior (dense muscle area). EMG signal crosstalk would overpredict the muscle forces of less active muscles and underpredict the net moments. This would increase the estimated co-contraction, and, consequently, increase the estimated spinal compressive force. Another possible limitation is that no distinctions about the mechanical functions of different muscles were made in spite of the functional differentiation in the muscles. By using surface electrodes, grouping of the muscles was inevitable. This forces an assumption that the muscles of the same group are the same in their EMG (% MVC) activities and functions. There are insufficient data to separate the detailed neural activation and functions of muscles within a group.

The concept that the muscle force is proportional to cross-sectional area of the muscle should be considered carefully. The cross-section was made perpendicular to the superior axis. But, in some muscles, the directions of muscle fibers are not parallel with the superior axis. One must depend on anatomical accuracy to satisfy the moment equilibrium requirements about all three joint axes simultaneously (McGill, 1992). Individualized anatomic data will make the results more accurate and reliable. But, linear geometric scaling of the cross-sectional anatomic data is one of the reasonable attempts when the individual anatomical data are not available.

The validation of the model is still problematic because there is no direct way to measure the muscle forces. The correlation of predicted muscle forces with EMG amplitudes is usually used as evidence of validity of spine models, specifically optimization models. Since the EMGAO model uses the EMG amplitudes as its model-input values, the EMGAO model has inherent physiological validity. Another way to estimate the accuracy of the model is to calculate the errors in the external moments predicted by the model. In this study, the model showed the fairly small RMS errors (14.2%) during all trials about all three orthogonal axes.

Foust et al. (1973) investigated the effects of gender, age and stature on cervical muscle strength with a group of 180 volunteers chosen on the basis of gender, age (18-74 years), and stature. In their study, the average muscle strength of males was greater than that of females in every age and stature group, and gender also seemed to influence the effects of age. On the average, females were only 60 % as strong as males. Over the adult lifespan, voluntary strength capability diminishes by 25 %. In this study, the age and gender effects were not considered. The maximum muscle force generated per unit of cross-section

area (physiologic muscle strength) might need to vary according to age and gender. Future study may develop cervical model with dynamic loading conditions including the effects of muscle length change and the rate of muscle length change. A more extensive study with varying postures would also be helpful to expand the biomechanical knowledge of the cervical spine.

The EMGAO approach showed its capability of balancing moments and sensitivity to small variation in muscle response. The EMGAO model estimated a substantial variation of muscle force distribution patterns that corresponded to various EMG activation patterns of neck musculature including antagonistic co-contractions. The spinal compressive loads at C4/5 level calculated in this study were higher than previously indicated (Moroney et al., 1988) by approximately 12% in extension, 81% in flexion, and 19% in left lateral bending. These higher physiological loads at C4/5 level must be considered possible during orthopedic reconstruction at this level. In addition, this knowledge will be useful for diagnostic, surgical, preventive, and rehabilitative medicine.

References

Butchthal, F. and Schmalbruch, H., 1970, "Contraction times and fibre types in intact human muscle," *Acta Physiol. Scand.* Vol. 79, pp. 435~452.

Choi, H., Vanderby, R., 1999, "Comparison of Biomechanical Human Neck Models: Muscle Forces and Spinal Loads at C4/5 Level," *J. Appl. Biomech.* Vol. 15-2, pp. 120~138.

Cholewicki, J. and McGill, S. M., 1994, "EMG assisted optimization: hybrid approach for estimating muscle forces in an indeterminate biomechanical model," *J. Biomech.* Vol. 27(10), pp. 1287~1289.

Cholewicki, J., Panjabi, M. M., and Khachatryan, A., 1997, "Stabilizing function of trunk flexor-extensor muscles around a neutral spine posture," *Spine* Vol. 22(19), pp. 2207~2212.

Cholewicki, J., McGill, S. M., and Norman, R. W., 1995, "Comparison of muscle forces and joint load from an optimization and EMG assisted lumbar spine model: towards development of hybrid approach," *J. Biomech.* Vol. 28(3), pp. 321~331.

Clauser, C. E., McConville, J. T., and Young, J. W., 1969, "Weight, volume, and center of mass of segments of the human body," *Wright-Patterson Air Force Base, Ohio*, pp. AMRL-TR-69~70.

Foust, D. R., Chaffin, D. B., Snyder, R. G., and Baum, J. K., 1973, "Cervical range of motion and dynamic response and strength of cervical muscles," *Proceedings of the 17th Stapp Car Crash Conference*, SAE Paper 73075, pp. 285~308.

Gardner-Morse, M. G. and Stokes, I. A., 1998, "The effects of abdominal muscle coactivation on lumbar spine stability," *Spine* Vol. 23(1), pp. 86~92.

Hof, A. L., 1984 "EMG and muscle force: an introduction," *Human Movement Science* Vol. 3, pp. 119~153.

Kim, S. and Pandy, M. G., 1998, "An Optimal Control Model for Determining Articular Contact Forces at the Human Knee During Rising from a Static Squat Position," *KSME Int'l. Journal in Korea* Vol. 12, No. 5, pp. 847~858.

Ladin, Z., Murthy, K. R., and Deluca, C. J., 1989, "Mechanical Recruitment of Low-Back Muscles," *Spine* Vol. 14, pp. 927~938.

Maiman, D. J., Snaces, A. J., Myklebust, B., Larson, S. J., Houterman, C., Chilbert, M., and El-Ghatit, A. Z., 1983, "Compression Injuries of the Cervical Spine: A Biomechanical Analysis," *Neurosurgery* Vol. 13, pp. 254~260.

Marras, W. S., 1988, "Predictions of Forces Acting Upon the Lumbar Spine Under Isometric and Isokinetic Conditions: A Model Experiment Comparison," *Int. J. Ind. Ergonomics* Vol. 3, pp. 19~27.

McGill, S. M. and Norman, R. W., 1986, "Partitioning of the L4/L5 Dynamic Moment into Disc, Ligamentous, and Muscular Component During Lifting," *Spine* Vol. 11, pp. 666~678.

McGill, S. M., 1992 "A MyoelEctrically Based Dynamic Three-Dimensional Model to Predict Loads on Lumbar Spine Tissues During Lateral

Bending," *J. Biomech.* Vol. 25, pp. 395~414.

McGill, S. M., 1991, "Electromyographic Activity of the Abdominal and Low Back Musculature During the Generation of Isometric Dynamic Axial Trunk Torque: Implications for Lumbar Mechanics," *J. Orthop. Res.* Vol. 9, pp. 91~103.

Milner-Brown, H. S., Stein, R. B., and Yemm, R., 1973, "The Contractile Properties of Human Motor Units During Voluntary Isometric Contractions," *J. Physiol.* Vol. 228, pp. 285~306.

Moroney, S. P., Schultz, A. B., and Miller, J. A. A., 1988, "Analysis and Measurement of Neck Loads," *J. Orthop. Res.* Vol. 6, pp. 713~720.

Olney, S. J. and Winter, D. A., 1985, "Predictions of Knee and Ankle Moments of Force in Walking from EMG and Kinematic Data," *J. Biomech.* Vol. 18, pp. 9~20.

Potvin, J. R. and Norman, R. W., 1993, "Quantification of Erector Spinae Muscle Fatigue During Prolonged, Dynamic Lifting Tasks," *Europ. J. Appl. Physiol. and Occup. Physiol.* Vol. 67, pp. 554~562.

Schultz, A. B. and Andersson, G. B. J., 1981, "Analysis of Loads on the Lumbar Spine," *Spine* Vol. 6, pp. 76~82.

Schultz, A. B., Andersson, G. B. J., Haderspeck, K., Örtengren, R., Nordin, M., and Bjork, R., 1982a, "Analysis and Measurements of Lumbar Trunk Loads in Tasks Involving Bends and Twists," *J. Biomech.* Vol. 15, pp. 669~675.

Schultz, A. B., Andersson, G. B. J., R., Bjork, R., and Nordin, M., 1982b, "Analysis and Quantitative Myoelectric Measurements of Loads on the Lumbar Spine when Holding Weights in Standing Postures," *Spine* Vol. 7, pp. 390~397.

Schultz, A. B., Cromwell, R., Warwick, D., and Andersson, G. B. J., 1987, "Lumbar Trunk Muscle Use in Standing Isometric Heavy Exertions," *J. Orthop. Res.* Vol. 5, pp. 320~326.

Schultz, A. B., Haderspeck, K., Warwick, D., and Portillo, D., 1983, "Use of Lumbar Trunk Muscles in Isometric Performance of Mechanically Complex Standing Tasks," *J. Orthop. Res.* Vol. 1, pp. 77~91.

Shea, M., Edwards, W. T., White, A. A., and Hayes, W. C., 1991, "Variations of Stiffness and Strength Along the Human Cervical Spine," *J. Biomech.* Vol. 24, pp. 95~107.

Son, K. and Miller, J. A. A., 1993, "Trunk and Lower Extremity Muscle Activity in Seated Weight-Moving Tasks: Three-Dimensional Analyses of Intersubject and Intertask Differences," *KSME Journal in Korea* Vol. 7, No. 4, pp. 372~388.

Stokes, I. A. F., Rush, S., Moffroid, M., Johnson, G. B., and Haugh, L. D., 1987, "Trunk Extensor EMG-Torque Relationship," *Spine* Vol. 12, pp. 770~776.

Thelen, D. G., Schultz, A. B., and Ashton-Miller, J. A., 1995 "Co-Contraction of Lumbar Muscles During the Development of Time-Varying Triaxial Moments," *J. Orthop. Res.* Vol. 13 (3), pp. 390~398.

Vink, P., Daanen, H. A. M., and Verbout, A. J., 1989, "Specificity of Surface-EMG on the Intrinsic Lumbar Back Muscles," *Human Mov. Sci.* Vol. 8, pp. 67~78.

Vink, P., van der Velde, E. A., and Verbout, A. J., 1987 "A Functional Subdivision of the Lumbar Extensor Musculature," *Electromyogr. Clin. Neurophysiol.* Vol. 27, pp. 517~525.